

## Bearing Fault Diagnosis Method Using Envelope Analysis and Euclidean Distance

Haiping Li<sup>1</sup>, Jianmin Zhao<sup>1</sup>, Xinghui Zhang<sup>\*1</sup>, Hongzhi Teng<sup>1,2</sup>,  
Ruifeng Yang<sup>1</sup>, Lishan Hao<sup>3</sup>

<sup>1</sup>Mechanical Engineering College, Shijiazhuang, China

<sup>2</sup>Lanzhou Equipment Maintenance Center, Lanzhou, China

<sup>3</sup>Shijiazhuang Army Command College, China

\*Corresponding author, e-mail: [dynamicbnt@gmail.com](mailto:dynamicbnt@gmail.com)

### Abstract

*Bearings are widely used in rotating machines. Its health status is a significant index to indicate whether machines run continually or not. Detecting the bearing faults timely is very important for the maintenance decision making. In this paper, a new fault diagnosis method based on envelope analysis and Euclidean Distance is developed. Envelope analysis is used to enable the fault frequencies clearly. Then, amplitudes of fault frequencies are used as the fault features. Finally, Euclidean Distance is used to identify the different fault types. This method can identify the fault locations intelligently even if the bearings are under different fault levels. The effectiveness of this methodology is demonstrated using the bearing data sets of Case Western Reserve University.*

**Keywords:** bearing, fault diagnosis, envelope analysis, euclidean distance

**Copyright © 2014 Institute of Advanced Engineering and Science. All rights reserved.**

### 1. Introduction

Researchers pay great attention to rolling element bearings because they are key components of mechanical systems and always play important roles in mechanical transmission. Proper functioning of mechanical systems depends on the smooth and normal running of the bearings. Therefore, bearing fault diagnosis is very important to prevent the machine break down and save costs. Generally, two techniques are commonly used to diagnose the bearing faults: model-based methods, and data-driven methods. In model-based methods, the goal of signal models (such as wavelet analysis [1], morphological theory [2]) are to find the fault frequencies of different locations (like inner race, out race, ball, and cage). In practice, it is impossible to store all the vibration signals for vibration analysis. On the contrary, data-driven methods can diagnose the bearing faults using features extracted from the vibration signals without the demand to store a large amount of data.

Boutros and Liang [3] developed a discrete Hidden Markov Model (HMM) to determine the fault location and classify the fault severity. In this paper, energies of five frequency bands were used as the fault features. Kang and Zhang [4] used a continuous HMM to detect the incipient faults. Zhang etc. [5] proposed a method called ensemble empirical mode decomposition (EEMD) and distributing fitting testing in order to alleviate the mode mixing problem and choose useful IMFs, where EEMD is an improved technique of empirical mode decomposition (EMD). Like HMM, Support Vector Machine (SVM) [6-8], Wavelet Transform (WT) [9] and Artificial neural network (ANN) [10, 11] were widely used in bearing fault diagnosis. In these models, fault features are the key factors affecting the model performance. Therefore, in bearing fault diagnosis, extracting good features is a more important thing than model selection. Recently, many researchers pay main attention to the fault feature extraction methods. For bearing fault diagnosis, the research goal is to enhance the impulsive contents in the signal and depress the noise. Many novel method such as Spectral Kurtosis [12, 13], Minimum Entropy Deconvolution (MED) [13], etc. were developed for bearing fault diagnosis. Recently, a adaptive morphological gradient lifting wavelet was proposed in [14] for detecting the bearing defects. In this paper, the updating filters can be appropriately selected based on the local features in the signal. This enabled the fault characteristic frequency of bearing can be detected effectively. Morphology theory was used to diagnose the bearing fault and attracted

considerable attention for a long time. Raj and Murali [15] proposed a new algorithm in which the structuring elements was selected based on kurtosis. This enabled the morphological operators more robust for bearing fault diagnosis.

However, features extracted using above mentioned methods are very effective to determine the fault location under the assumption that training sets and test sets are collected from the same fault severity bearing produced by the same factory. In engineering practice, there will have many severity levels fault bearings waiting to be classified. Therefore, the training sets and test sets will be different. Some traditional feature extraction methods will be ineffective in this circumstance. In order to solve this dilemma, this paper developed a new fault diagnosis method based on envelope analysis and Euclidean Distance.

## 2. Euclidean Distance

Euclidean Distance Method is one of the pattern recognition methods widely used in image processing. Assume there are two samples  $X_i, X_j$ . They can be denoted as:

$$X_i = \begin{pmatrix} x_{i1} \\ x_{i2} \\ \vdots \\ x_{in} \end{pmatrix} = (x_{i1}, x_{i2}, \dots, x_{in})^T, X_j = \begin{pmatrix} x_{j1} \\ x_{j2} \\ \vdots \\ x_{jn} \end{pmatrix} = (x_{j1}, x_{j2}, \dots, x_{jn})^T \quad (1)$$

Figure 1(a) shows that these two samples are belong to same class because the distance between them is very short. On the contrary, these two samples are belong to different classes due to its long distance as depicted in Figure 1(b).

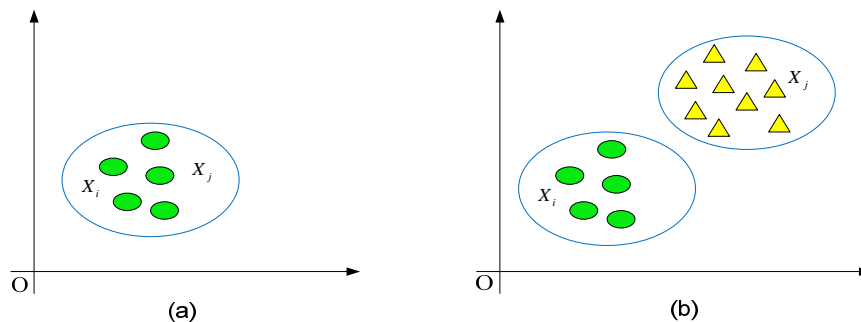


Figure 1. The Sketch Map of the Distance between Samples: (a) same class, (b) different class

The Euclidean Distance can be defined as:

$$D_{ij}^2 = (X_i - X_j)^T (X_i - X_j) = \|X_i - X_j\|^2 = \sum_{k=1}^n (X_{ik} - X_{jk})^2 \quad (2)$$

It is assumed that there are  $M$  classes:  $\omega_1, \omega_2, \dots, \omega_M$ . Each class contains  $n$  samples. For example, the  $\omega_i$  class can express as  $X(\omega_i) = (X_1(\omega_i), X_2(\omega_i), X_3(\omega_i), \dots, X_n(\omega_i))^T$ . If we want to know which class the vector  $X = (x_1, x_2, x_3, \dots, x_n)$  belongs to, the distances between this vector to every classes need to be calculated.

$$d^2(X, \omega_i) = \left( X - \overline{X^{(\omega_i)}} \right)^T \left( X - \overline{X^{(\omega_i)}} \right) \quad (3)$$

$\overline{X^{(\omega_i)}}$  is the center of the  $\omega_i$ .

Then, all the distances are compared.

$$d\left(X, \overline{X^{(e_i)}}\right) < d\left(X, \overline{X^{(e_j)}}\right), \quad j = 1, 2, L, M, i \neq j \quad (4)$$

Finally, which class this vector belongs to can be know.

### 3. Framework of the Proposed Method

The proposed method is made up of two stages: training and diagnosis. It can be seen in Figure 2.

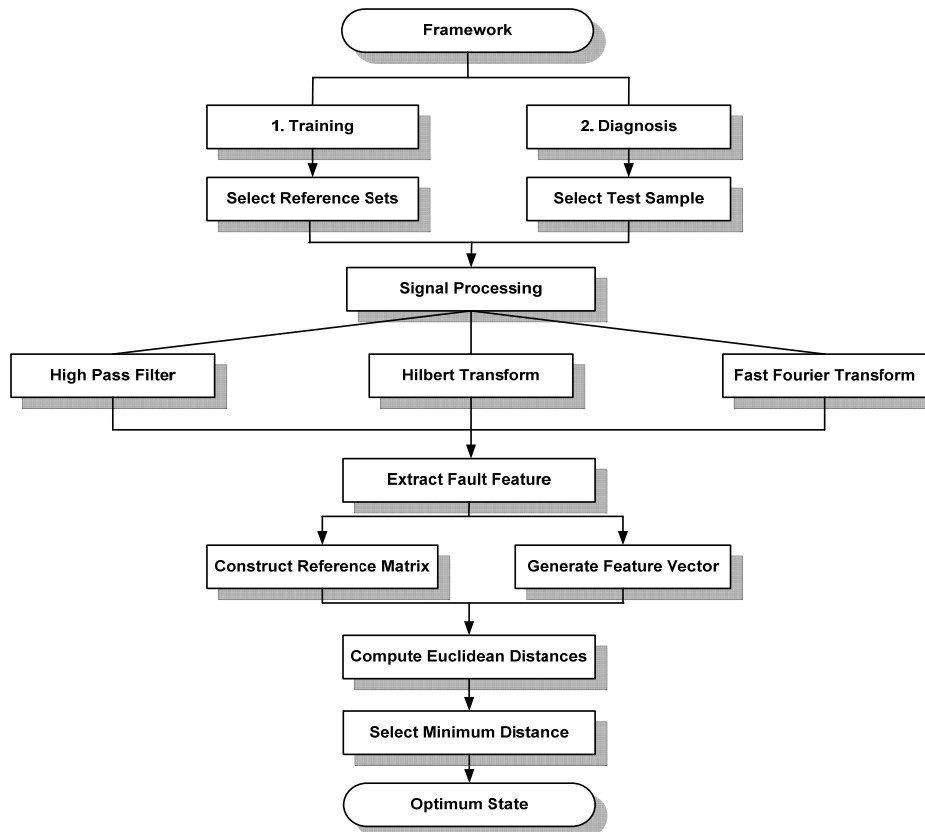


Figure 2. Framework of the Proposed Method

For saving time, some steps of diagnosis can be done ahead of schedule. Such as select test sample, signal processing, and extract fault feature. The procedure also can be explained as follows.

Step 1. Select reference sets, represent bearing faults location (inner race, ball, and outer race), and test sample which the state is unknown.

Step 2. Due to the amplitude modulation of the bearing vibration, its frequency spectrum consists of some interferential signals. So demodulation is necessary. In this paper, high pass filter, Hilbert transform, and the Fast Fourier transform (FFT) are used (these are the necessary steps of envelope analysis). The reason for using them will be described in next section.

Step 3. Fault feature selection is very important to final results. Amplitudes of fault frequencies (inner raceway, ball, and outer raceway) are used as the feature vector in this study.

Step 4. Construct reference matrix using the three fault vectors. At the same time, generate feature vector of test sample. All of the vectors are consist of the three numbers obtained above.

Step 5. Compute the Euclidean distances between the test sample and each vector in the reference matrix.

Step 6. Select the minimum distance and its corresponding state is the optimum state of the test sets.

## 4. Data Analysis and Discussion

### 4.1. Data Specifications

The data utilized in this study is obtained from the Case Western Reserve University Bearing Data Center [16]. The Electro-Discharge Machining (EDM) method is used to introduce faults to test bearings. And the faults were planted at different positions (inner raceway, ball, and outer raceway). Because fault locations at the outer raceway were fixed relatively, so the damaged point located in different areas of outer raceway would make directive affect on bearing system. So, the fault locations were machined at positions equivalent to 6:00 o'clock, 12:00 o'clock, and 3:00 o'clock time configuration. Meanwhile, the diameters of faults range from 0.007" to 0.028". Two types' bearing (SKF and NTN) were used to detect different fault level. The NTN bearings are only used for fault diameter 0.028". The rotary speed contains 1,797 rpm, 1,772rpm, 1,750rpm, and 1,730rpm. And sampling frequency are 12,000Hz and 48,000Hz. Vibration data was recorded using motor loads of 0-3 hp. And the monitoring parts are drive end (DE) and fan end (FE).

Due to the limit space, a partial data was utilized in this paper, monitoring at DE, collect at 12,000 samples/s, 6205-2RS JEM SKF, deep groove ball bearing which the fault diameters of them are 0.007", 0.014", and 0.021". At the same time, the faults locations detected were at the inner raceway, ball, and 6:00 o'clock time configuration of outer raceway. The rotary speed and motor load are all contained. Table 1 shows the utilized data in this paper. In the table, 'X' indicates data available.

Table 1. The List of Data Used in this Paper

Case no.	Fault diameter	Motor load(hp)	Motor speed(rpm)	Inner race	Ball	Outer race
1	0.007"	0	1797	X	X	X
2	0.007"	1	1772	X	X	X
3	0.007"	2	1750	X	X	X
4	0.007"	3	1730	X	X	X
5	0.014"	0	1797	X	X	X
6	0.014"	1	1772	X	X	X
7	0.014"	2	1750	X	X	X
8	0.014"	3	1730	X	X	X
9	0.021"	0	1797	X	X	X
10	0.021"	1	1772	X	X	X
11	0.021"	2	1750	X	X	X
12	0.021"	3	1730	X	X	X

### 4.2 Model training

MATLAB signal processing toolbox is mainly used in this study. Figure 3(a) shows the frequency spectrum of original signal ((a), (b), and (c) are all take test sample 105 as example).

An obvious phenomena of fault bearings is exist fault characteristic frequency and its multi-frequencies in amplitude spectrum. Fault characteristic frequency of bearings is related to the resonance frequency with housing, and usually appear at high frequency region. So the fault characteristic frequency value of bearings will be different along with housing changing even at the different positions of the same machine, maybe sometimes at 4,000Hz and sometimes at 5500Hz. Thus extract feature from original signal directly (like [3], select energies of five frequency bands as feature) can not get exact results. For the above reason, envelope analysis is used in this paper. Through this technique, the values of fault characteristic frequencies are all less than 200. The influence of modulation signal will be reduced to minimal.

At the beginning of using envelope analysis technique, Hilbert transform should be implemented to obtain analytical signal. Then the envelope of signal can be computed.

Assume the original signal is  $x(t)$ , the Hilbert transform of it can be defined as:

$$\hat{x}(t) = H\{x(t)\} = \frac{1}{\pi} \int_{-\infty}^{\infty} \frac{x(\tau)}{t-\tau} d\tau \quad (5)$$

Combine signal  $x(t)$  and  $\hat{x}(t)$  can get the analytical signal  $z(t)$ .

$$z(t) = x(t) + i \cdot \hat{x}(t) \quad (6)$$

Then, the envelope of  $x(t)$  can be computed by equation (7).

$$Env_x(t) = \sqrt{x^2(t) + \hat{x}^2(t)} \quad (7)$$

After processed by Hilbert transform technique, the signal is a discrete series of numbers. Discrete Fourier Transform (DFT) is needed to computing the signal frequency spectrum. For the purpose of reducing the amount of computations involved in the DFT, the Fast Fourier Transform (FFT) is used in this study.

Figure 3(c) shows the envelope spectrum. The function of envelope analysis technique can be seen obviously. Noisy signal was depressed to a great extent. However, original fault characteristic frequency will not be found at low frequency region, in the interest of avoiding unnecessary disturb, a high pass filter is designed at first to filtrating the frequency under 900Hz. The signal after filter can be seen in Figure 3(b).

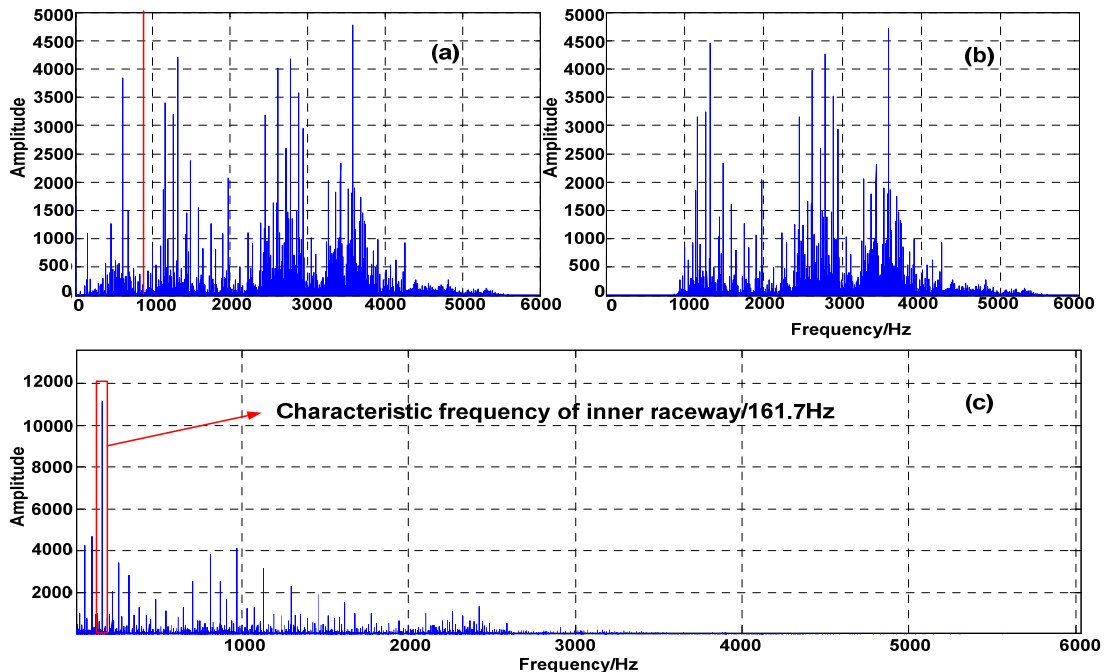


Figure 3. The Results of Every Process: (a) original signal, (b) the signal after filter, and (c) envelope spectrum

Every fault location has a fixed characteristic fault frequency, the frequencies can be computed by Equation (8-10).

$$F_o = \frac{F_R}{2} N_B \left( 1 - \frac{D_B \cos \alpha}{D_p} \right) \quad (8)$$

$$F_i = \frac{F_R}{2} N_B \left( 1 + \frac{D_B \cos \alpha}{D_p} \right) \tag{9}$$

$$F_B = \frac{D_p}{D_B} F_R \left( 1 - \frac{D_B^2 \cos^2 \alpha}{D_p^2} \right) \tag{10}$$

Where  $F_O, F_I, F_B$  are the fault characteristic frequencies of outer raceway, inner raceway, and ball.  $F_R$  is the bearing rotational frequency,  $N_B$  is the roller number,  $\alpha$  is the contact angle,  $D_B$  is the roller diameter, and  $D_C$  is roller pitch diameter. The bearing information of the bearings this paper used are shown in Table 2.

Table 2. Bearing Information (6205-2RS JEM SKF, deep groove ball bearing)

Ball Diameter	Size(inches)		Defect frequencies(multiple of running speed in Hz)		
	Pitch Diameter		Outer Ring	Inner Ring	Rolling Element
0.3126	1.537		3.5848	5.4152	4.7135

The frequencies are also allowed to change in a certain range. In this study, the range is defined  $\pm 2$  around the fault frequency of inner race, ball, and outer race. Then the characteristic matrix of reference sets is constructed by the three numbers.

Finally, the reference sets should be selected. Here, the sample 108, 121, and 133 are chosen. Then the Euclidean Distances between test sample and each vector in the reference matrix can be computed, as Figure 4 shows. In order to illustrate, three test sample, 105, 118, and 130 are selected.

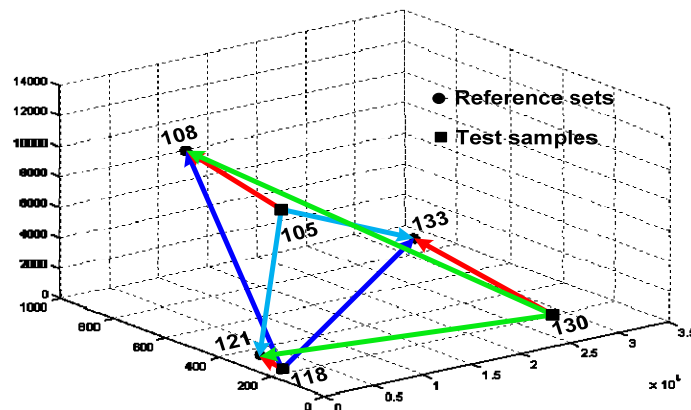


Figure 4. Distances between Test Samples and Reference Sets

In the Figure 4, sample 108, 121, and 133 represent three fault locations (inner race, ball and outer race). Lines represent the distances between two samples, and the red line is the shortest. The optimum state of test sample is easy to detect.

### 4.3. Fault Diagnosis and Results Analysis

After a sequence of processes, the results appear. Table 3 shows the distances between test samples and reference sets. The detected fault locations also can be seen in it.

In the table, the minimum numbers (in bold) represent the optimum state of test samples. And the words written in red and italic indicate that the detected fault locations do not accord with predicted positions. The accurate rate of this method is approximate 88%.

Table 3. Distances between Test Samples and Reference Sets

Case no.	Fault description		Distances with reference sets			Detected fault location
	Diameter	Location	Inner race(108)	Ball(121)	Outer race(133)	
1.(105)	0.007"	Inner race	<b>4.8328E+03</b>	1.0699E+04	1.9093E+04	Inner race
2.(106)	0.007"	Inner race	<b>4.5968E+03</b>	1.0461E+04	1.8994E+04	Inner race
3.(107)	0.007"	Inner race	<b>4.6936E+03</b>	1.0558E+04	1.9056E+04	Inner race
4.(169)	0.014"	Inner race	<b>1.1379E+03</b>	4.7892E+03	1.6204E+04	Inner race
5.(170)	0.014"	Inner race	<b>1.3929E+03</b>	4.5575E+03	1.5997E+04	Inner race
6.(171)	0.014"	Inner race	<b>2.1944E+03</b>	3.7079E+03	1.5869E+04	Inner race
7.(172)	0.014"	Inner race	<b>2.4364E+03</b>	3.4487E+03	1.5885E+04	Inner race
8.(209)	0.021"	Inner race	<b>9.1596E+03</b>	1.5022E+04	2.1601E+04	Inner race
9.(210)	0.021"	Inner race	<b>1.0638E+04</b>	1.6502E+04	2.2698E+04	Inner race
10.(211)	0.021"	Inner race	<b>1.3475E+04</b>	1.9337E+04	2.4738E+04	Inner race
11.(212)	0.021"	Inner race	<b>9.3616E+03</b>	1.5220E+04	2.1590E+04	Inner race
12.(118)	0.007"	Ball	5.8181E+03	<b>3.8999E+02</b>	1.5221E+04	Ball
13.(119)	0.007"	Ball	5.5417E+03	<b>5.2720E+02</b>	1.5215E+04	Ball
14.(120)	0.007"	Ball	5.0408E+03	<b>1.4182E+03</b>	1.4603E+04	Ball
15.(185)	0.014"	Ball	6.1108E+03	<b>4.2060E+02</b>	1.5493E+04	Ball
16.(186)	0.014"	Ball	6.0537E+03	<b>3.6241E+02</b>	1.5381E+04	Ball
17.(187)	0.014"	Ball	6.0687E+03	<b>2.6890E+02</b>	1.5571E+04	Ball
18.(188)	0.014"	Ball	6.1330E+03	<b>3.4545E+02</b>	1.5559E+04	Ball
19.(222)	0.021"	Ball	4.6866E+03	<b>1.2598E+03</b>	1.5555E+04	Ball
20.(223)	0.021"	Ball	5.2242E+03	<b>8.1954E+02</b>	1.5524E+04	Ball
21.(224)	0.021"	Ball	5.2459E+03	<b>7.0211E+02</b>	1.5335E+04	Ball
22.(225)	0.021"	Ball	5.5203E+03	<b>3.6028E+02</b>	1.5558E+04	Ball
23.(130)	0.007"	Outer race	2.8371E+04	2.7623E+04	<b>1.2029E+04</b>	Outer race
24.(131)	0.007"	Outer race	3.3187E+04	3.2528E+04	<b>1.6929E+04</b>	Outer race
25.(132)	0.007"	Outer race	3.0518E+04	2.9865E+04	<b>1.4270E+04</b>	Outer race
26.(197)	0.014"	Outer race	5.8335E+03	<b>6.2926E+01</b>	1.5630E+04	Ball
27.(198)	0.014"	Outer race	5.7549E+03	<b>1.4082E+02</b>	1.5648E+04	Ball
28.(199)	0.014"	Outer race	5.7740E+03	<b>1.7034E+02</b>	1.5479E+04	Ball
29.(200)	0.014"	Outer race	5.9774E+03	<b>1.5577E+02</b>	1.5683E+04	Ball
30.(234)	0.021"	Outer race	2.5356E+04	2.4673E+04	<b>9.0970E+03</b>	Outer race
31.(235)	0.021"	Outer race	1.8135E+04	1.7165E+04	<b>1.6617E+03</b>	Outer race
32.(236)	0.021"	Outer race	2.3676E+04	2.2958E+04	<b>7.3863E+03</b>	Outer race
33.(237)	0.021"	Outer race	2.4307E+04	2.3632E+04	<b>8.0698E+03</b>	Outer race

\*Note: The numbers after case no. are samples' name.

## 5. Conclusion

Rolling elements bearings are the most essential parts in rotating machinery. So, bearing diagnosis and fault location detect is very important in engineering practice. A fast and accuracy way to identify the state of bearings is seriously needed for the maintenance decision making. In this paper, a new fault diagnosis method based on envelope analysis and Euclidean Distance is developed. The effectiveness of this methodology is demonstrated using the bearing data sets of Case Western Reserve University. Compare to other methods utilized in resolving this issue, the approach this paper used is very convenient and intelligent. This method can indentify the fault location well and truly even if the bearings are under different fault levels. And the training procedure costs only about 1s. Meanwhile, the success rate of the method is approximate 88%.

## References

- [1] Jiang YH, Tang BP, Qin Y, Liu WY. Feature extraction method of wind turbine based on adaptive Morlet wavelet and SVD. *Renewable Energy*. 2011; 36(8): 2146-2153.
- [2] Wang J, Xu GH, Zhang Q, Liang L. *Application of improved morphological filter to the extraction of impulsive attenuation signals*. Mechanical Systems and Signal Processing. 2009; 23(1): 236-245.
- [3] Boutros T, Liang M. Detection and diagnosis of bearing and cutting tool faults using Hidden Markov models. *Mechanical Systems and Signal Processing*. 2011; 25(6): 2012-2124.
- [4] Kang JS, Zhang XH. Application of Hidden Markov Models in machine fault diagnosis. *Information-An International Interdisciplinary Journal*. 2012; 15(12B): 5829-5838.
- [5] Zhang YP, Zhang T, Teng J, Su HS. Improved Ensemble Empirical Mode Decomposition for rolling bearing fault diagnosis. *TELKOMNIKA Indonesian Journal of Electrical Engineering*. 2014; 12(1), DOI: 10.11591/telkomnika.v12i1.2928.
- [6] Kumar H, Kumar TAR, Amarnath M, Sugumaran V. Fault diagnosis of antifricition bearings through sound signals using support vector machine. *Journal of vibroengineering*. 2012; 14(4): 1601-1606.

- 
- [7] Konar P, Chattopadhyay P. Bearing fault detection of induction motor using wavelet and Support Vector Machines (SVMs). *Applied Soft Computing*. 2011; 11(6): 4203-4211.
- [8] Abbasion S, Rafsanjani A, Farshidianfar A, Irani N. Rolling element bearings multi-fault classification based on the wavelet denoising and support vector machine. *Mechanical Systems and Signal Processing*. 2007; 21(7): 2933-2945.
- [9] Li H, Yin YJ. Bearing fault diagnosis based on Laplace Wavelet Transform. *TELKOMNIKA Indonesian Journal of Electrical Engineering*. 2012; 10(8): 2139-2150.
- [10] Yu Y, Yu DJ, Chen JS. A roller bearing fault diagnosis method based on EMD energy entropy and ANN. *Journal of Sound and Vibration*. 2006; 294(1-2): 269-277.
- [11] Wang HQ, Chen P. Intelligent diagnosis method for rolling bearing faults using possibility theory and neural network. *Computers & Industrial Engineering*. 2011; 60(4): 511-518.
- [12] Chen BQ, Zhang ZS, Zi YY, He ZJ, Sun C. Detecting of transient vibration signatures using an improved fast spatial-spectral ensemble kurtosis kurtogram and its applications to mechanical signature analysis of short duration data from rotating machinery. *Mechanical Systems and Signal Processing*. 2013; 40(1): 1-37.
- [13] Sawalhi N, Randall RB, Endo H. The enhancement of fault detection and diagnosis in rolling element bearings using minimum entropy deconvolution combined with spectral kurtosis. *Mechanical Systems and Signal Processing*. 2007; 21(6): 2616-2633.
- [14] Li B, Zhang PL, Mi SS, Hu RX, Liu DS. An adaptive morphological gradient lifting wavelet for detecting bearing defects. *Mechanical Systems and Signal Processing*. 2012; 29(5): 415-427.
- [15] Rai AS, Murali N. Early classification of bearing faults using morphological operators and fuzzy inference. *IEEE Transactions on industrial electronics*. 2013; 60(2): 567-574.
- [16] Case Western Reserve University bearing data center. *12k Drive End Bearing Fault Data*. <<http://www.eecs.cwru.edu/laboratory/bearing/>>. 2013.